JACS
JOURNAL OF THE AMERICAN CHEMICAL SOCIETY
pubs.acs.org/JACS
Article

Anisotropic Dynamics and Mechanics of Macromolecular Crystals Containing Lattice-Patterned Polymer Networks

Kenneth Han, Jake B. Bailey, Ling Zhang, and F. Akif Tezcan*

Cite This: https://dx.doi.org/10.1021/jacs.0c10065
Read Online

ABSTRACT: The mechanical and functional properties of many crystalline materials depend on cooperative changes in lattice arrangements in response to external perturbations. However, the flexibility and adaptiveness of crystalline materials are limited. Additionally, the bottom-up, molecular-level design of crystals with desired dynamic and mechanical properties at the macroscopic level remains a considerable challenge. To address these challenges, we had previously integrated mesoporous, cubic ferritin crystals with hydrogel networks, resulting in hybrid materials (polymer-integrated crystals or PIX) which could undergo dramatic structural changes while maintaining crystalline periodicity and display efficient self-healing. The dynamics and mechanics of these ferritin-PIX were devoid of directionality, which is an important attribute of many molecular and macroscopic materials/devices. In this study, we report that such directionality can be achieved through the use of ferritin crystals with anisotropic symmetries (rhombohedral or trigonal), which enable the templated formation of patterned hydrogel networks in crystallo. The resulting PIX expand and contract anisotropically without losing crystallinity, undergo prompt bending motions in response to stimuli, and self-heal efficiently, capturing some of the essential features of sophisticated biological devices like skeletal muscles.

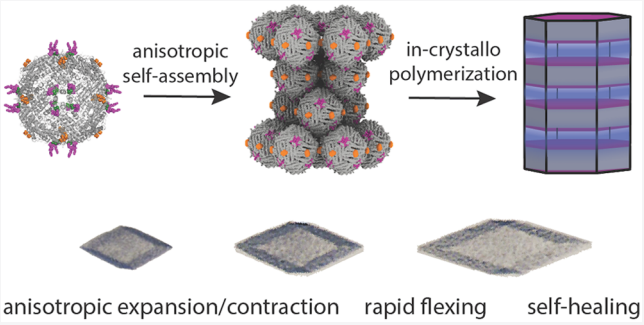

INTRODUCTION

A major goal in materials science is to apply chemical design at the atomic/molecular scale to generate collective structural, dynamic, and mechanical properties at the macroscopic scale.[1] The corresponding transfer and amplification of atomic/molecular-level information require the molecular building blocks to be organized and appropriately interconnected over multiple length scales.[2−4] Crystalline materials provide a distinct advantage in this regard in that they are composed of only one or few components arranged periodically, possessing both short and long-range order to allow structural and mechanical coupling in a cooperative manner. Indeed, there is a growing number of dynamic molecular crystals,[5,6] flexible protein lattices,[7,8] and porous framework materials,[9,10] which can promptly undergo dramatic lattice transformations and motions in response to external stimuli, with promising applications in actuation,[11−13] gas sorption and separation,[14−16] sensing,[17,18] and controlled release,[19,20] among others.[5,9,10] However, with relatively few but growing number of exceptions,[21−25] these dynamic crystalline materials tend to be brittle, cannot undergo large changes in volume at the macroscale without mechanical failure, or self-heal. These limitations are due to the fact that the lattice components need to be continuously interconnected during structural transformations to maintain crystallinity. While there have been advances in exploiting reticular chemistry approaches to deliberately design flexible porous networks,[26,27] the precise dynamic and responsive properties of molecular crystals are typically obtained *a posteriori* (rather than by *de novo* design) and on a case-by-case basis.[5,6] Consequently, the molecular building blocks or the self-assembly conditions cannot be easily altered to obtain different structural and mechanical properties at the macroscopic scale.

Soft polymeric materials like hydrogels provide a complete contrast to crystalline materials in many aspects. They are flexible, responsive, and their mechanical properties can be readily modulated by chemical design or physical manipulation.[28,29] However, these attributes are attained precisely because polymeric materials are devoid of the structural order and coherence of crystalline materials, leading ultimately to a lack of mechanical strength and cooperativity. Previously, we surmised that the complementary but mutually exclusive advantages of crystalline and polymeric materials (crystals: structural order/strength/cooperativity; hydrogels: flexibility/responsiveness/self-healing) could be combined if molecular crystals and hydrogel networks were chemically and structur-

Received: September 20, 2020

https://dx.doi.org/10.1021/jacs.0c10065
J. Am. Chem. Soc. XXXX, XXX, XXX−XXX

ally integrated.[30] As a proof-of-principle platform, we used the face-centered-cubic (*fcc*, *F*432 symmetry, $a \approx 180$ Å) crystals of the quasi-spherical, 24meric, iron-storage protein human H-chain ferritin (Figure 1a).[31,32] The cubic lattice is formed

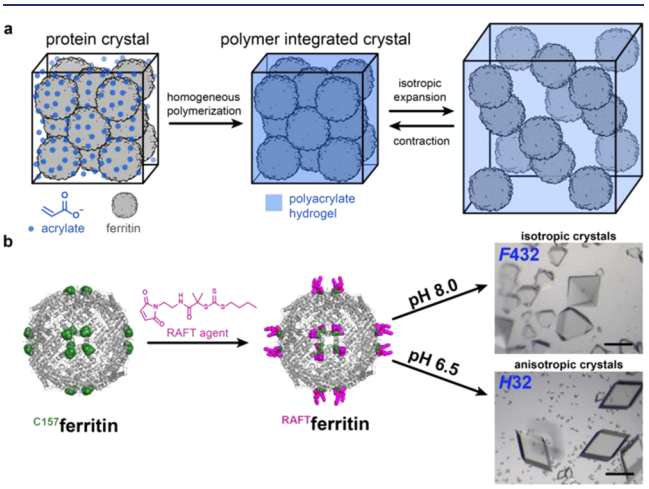

Figure 1. Ferritin as a building block for polymer-integrated crystals (PIX). (a) Schematic representation for the generation and isotropic expansion/contraction properties of cubic ferritin PIX homogeneously infused with a polyacrylate network.[30] (b) Schematic for the site-specific conjugation of a maleimide-functionalized RAFT agent to ^{C157}ferritin. The resulting conjugate, ^{RAFT}ferritin, can assemble into isotropic (cubic) or anisotropic (rhombohedral) crystals in a pH-dependent manner (scale bars: 100 μm).

through the Ca^{2+}-D84/Q86-mediated association of the C_2 symmetric interfaces of each ferritin molecule with 12 neighbors.[33] The ferritin lattice, like many protein crystals, is mesoporous, with continuously linked, nm-sized channels that account for an interstitial solvent content of 39%. This porosity allows the full permeation of ferritin crystals with acrylate polymer precursors and the subsequent formation of a pervasive polyacrylate (pA) hydrogel network within the lattice[30] (Figure 1a). Owing to the extensive noncovalent interactions between pA side chains and the surfaces of ferritin molecules, the resulting materials (termed Polymer-Integrated Crystals or PIX) behave essentially as singular chemical units that exhibit unprecedented material properties.[30] For example, pA-ferritin PIX can reversibly expand and contract in response to changes in ionic strength by nearly 600% in volume without losing crystalline order (Figure 1a) and display efficient self-healing. However, as a result of the uniform distribution and isotropic expansion/contraction of the pA network within the protein lattice, the structural dynamics of the first-generation ferritin-PIX were also isotropic, meaning that they lacked directionality.[30] Inspired by the remarkable mechanics of skeletal muscles, there has been extensive interest in designing anisotropic soft-material platforms that display directional motion and anisotropic mechanical properties.[34,35] Accordingly, we asked whether it is possible to control the spatial distribution of hydrogel networks within ferritin-PIX to achieve directional/anisotropic dynamic behavior. Here, we report that the hydrogel networks within PIX can indeed be patterned by the orientation and structural details of the distinct protein−protein interfaces in noncubic ferritin lattices. The resulting, anisotropic ferritin-PIX with lattice-patterned hydrogel networks display directional expansion/contraction and rapid bending motions, while retaining crystalline order, as well as chemical responsiveness and efficient self-healing behavior. The anisotropic ferritin-PIX thus provide a compelling example for the molecular-scale design of hierarchical materials with bespoke macroscale properties.

RESULTS AND DISCUSSION

Preparation, Characterization, and Self-Assembly of Ferritin Modified with RAFT Agents. To generate anisotropic ferritin-PIX, we set out to prepare a ferritin variant that was site-selectively modified with RAFT (reversible addition−fragmentation chain-transfer) agents.[36,37] Our rationale was based on our original expectation that the RAFT-modified ferritins could enable the controlled growth of polymer networks in spatially well-defined locations within the protein lattice. RAFT polymerization[36,37] provides excellent compatibility with aqueous solutions and acrylate monomers, does not require transition metal ions (which may interfere with ferritin self-assembly), and has been commonly used to generate covalent protein−polymer hybrids with high efficiency via graft-from strategies.[38,39] Accordingly, we synthesized a Cys-specific maleimide-functionalized trithiocarbonate RAFT agent (Figure 1b and S1). We used this agent to site-selectively label the ferritin variant, ^{C157}ferritin, which bears a single set of surface-exposed Cys residues (24 total, at positions 157) flanking the ferritin C_4 symmetry axes (Figure 1b and S2). The graft-from growth of the pA polymer from the modified variant (termed ^{RAFT}ferritin) could be induced by the radical initiators VA-044 or APS/TEMED and was confirmed by SDS-PAGE electrophoresis and gel permeation chromatography (GPC) (Figures S3 and S4).

We next examined the self-assembly of ^{RAFT}ferritin into 3D crystals. Under typical conditions used for Ca^{2+}-mediated ferritin crystallization (≥5 mM $CaCl_2$, pH 8.0), we obtained octahedron-shaped, *fcc* crystals (*F*432, a = 179.9 Å, PDB ID: 6WYF) of ^{RAFT}ferritin that were isomorphous with those of unmodified ^{C157}ferritin (Figures 1b and 2a). RAFT agents attached to the C157 side chains extend into the 6 nm wide, cube-shaped cavities in the lattice and can be discerned in the 1.25-Å resolution crystal structure up to the amide group (Figure 2a). When the solution pH is lowered to ≤6.5, ^{RAFT}ferritin molecules self-assemble into large (≥60 μm) rhombohedron-shaped crystals (*H*32, $a = b$ = 127.0 Å, c = 281.7 Å, PDB ID: 6WYG) which lack the 3D isotropy of the *fcc* crystals (Figures 1b and 2b).

The rhombohedral ^{RAFT}ferritin crystal lattice can be considered as a layered structure (Figure 2b). The hexagonal layers in the *ab*-plane are mediated by Ca^{2+}-D84/Q86 interactions between each ferritin molecule and six neighbors (Figure 2c), as in the cubic crystals. In contrast, the interlayer interactions along the *c*-axis are formed by contacts between the hydrophobic patches consisting of groups of four C157-RAFT moieties surrounding the ferritin C_4 axes (Figure 2d). These interactions further connect each ferritin molecule with six additional neighbors in the *c*-direction, yielding a quasi-hexagonal close-packed arrangement with a denser packing (interstitial solvent content = 32.5%) than the cubic crystals. Electrostatic calculations show that at pH = 8, C_4 surfaces of ferritin are highly negatively charged and thus self-repulsive, accounting for the *fcc* arrangement (Figure S5). Upon lowering the pH to ≤6.5, the negative charge is mostly mitigated, promoting hydrophobic interlayer interactions (Figure S5). Thus, although each ^{RAFT}ferritin molecule is inherently isotropic, the energetic balance/competition between different

https://dx.doi.org/10.1021/jacs.0c10065
J. Am. Chem. Soc. XXXX, XXX, XXX−XXX

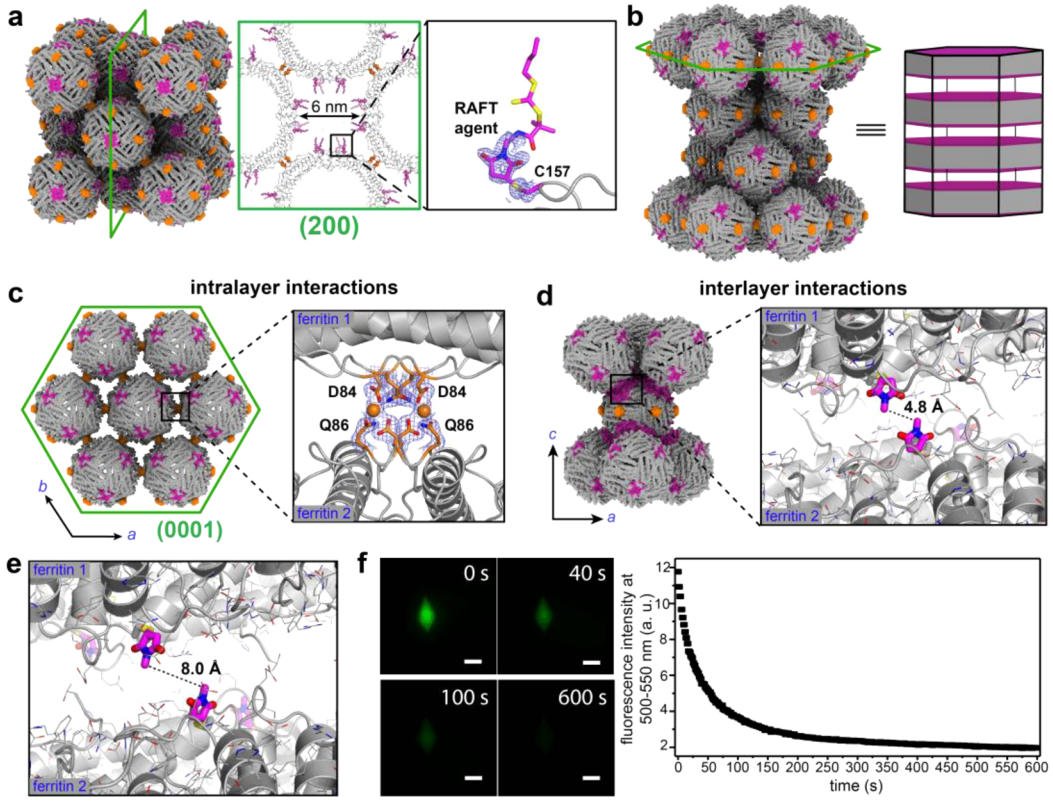

Figure 2. Formation and structural properties of ^{RAFT}ferritin crystals/PIX. Surface positions involved in Ca^{2+}-mediated ferritin-ferritin interactions at the ferritin C_2 axes are highlighted in orange and the RAFT-labeled C157 patches at the ferritin C_4 axes are shown in magenta. (a) The *fcc* (*F*432) packing arrangement of the isotropic ^{RAFT}ferritin crystals, along with a view of the lattice along the (200) plane and a close-up view of the RAFT agents (magenta) attached to C157 positions. The $2F_o-F_c$ electron density map for a single conformation of the RAFT-labeled C157 site is contoured at 0.7σ. (b) The hexagonal-layered (*H*32) packing arrangement of the anisotropic ^{RAFT}ferritin crystals. The (0001) plane is shown as a green hexagon. (c) Intralayer interactions between ferritin molecules in the (0001) plane oriented along the *ab*-plane are mediated by Ca^{2+} ions (orange spheres) and two pairs of D84 and Q86 side chains. (d) Interlayer interactions, oriented along the *c* axis, are mediated by ferritin surfaces that include hydrophobic patches (purple) formed by the RAFT agents. (e) Interlayer separation increases by *ca.* 3 Å after acrylate infusion. (f) Formation of the pA within rhombohedral ^{RAFT}ferritin crystals is monitored by confocal fluorescence microscopy (left) through the disappearance of pyranine fluorescence, which is complete within 10 min (right, scale bars: 100 μm).

interactions (metal-mediated and hydrophobic) governing its self-assembly yield both isotropic and anisotropic lattice arrangements in a condition-dependent manner, similar to what has been observed for spherical nanoparticles.[40,41]

Anisotropic Dynamics of Rhombohedral ^{RAFT}Ferritin PIX. There have been extensive efforts toward designing hydrogel-based materials that display muscle-like, directional motion, and complex deformations in response to external stimuli.[34,35] However, hydrogels inherently undergo isotropic volumetric changes.[34] Therefore, multistep physical alignment/patterning strategies and external fields have to be applied to introduce anisotropic arrangements of polymer chains or embedded particles to obtain directional behavior with hydrogels.[34,35,42−47] In our system, the anisotropic structure of the rhombohedral ^{RAFT}ferritin lattices and the specific positioning of the RAFT agents in these lattices create a unique opportunity to generate an anisotropic hydrogel network solely via (one-step) molecular self-assembly and potentially generate directional actuation.

To investigate this possibility, rhombohedral ^{RAFT}ferritin crystals were first perfused with 1 M of acrylate monomers, which caused no visible loss in the integrity of the crystals. Interestingly, single-crystal X-ray diffraction (sc-XRD) measurements indicated that this treatment caused a 10-Å expansion of the lattice along the *c* axis whereas the *a*/*b* dimensions increased by only 2 Å (unit cell: $a = b = 128.9$ Å, $c = 291.8$ Å, PDB ID: 6WYH). This behavior is quite similar to that of layered double hydroxide materials, which undergo anisotropic lattice expansion/contraction upon exchange of the intercalating anions in the interlayer spaces.[48] The 2.2-Å resolution structure of the acrylate-soaked ^{RAFT}ferritin revealed a striking picture in which the neighboring hexagonal ferritin layers (i.e., the *ab*-planes) were separated from one another by 3−4 Å (Figure 2e). This expansion eliminates any observable direct contact between the ferritin molecules along the *c* direction (and increases the interstitial solvent content of the lattice from 32% to 37%), while the Ca^{2+}-mediated intralayer interactions remain intact. These findings highlight the fluidity of the interlayer interactions and the anisotropy inherent in the rhombohedral crystals.

The formation of the pA hydrogel network within ^{RAFT}ferritin crystals was efficiently mediated by radical initiators VA-044 (0.2% w/v) or APS/TEMED (1% w/v). *In-crystallo* polymerization was monitored by confocal microscopy, whereby we followed the quenching of the fluorescence of pyranine molecules (λ_{max} = 512 nm) infused into the crystals (Figure 2f, S6, and Video S1). The process was typically complete in <2 min for a typical, 100 μm-sized crystal, but we incubated the acrylate-permeated ^{RAFT}ferritin crystals with radical initiators for at least 5 min to ensure full hydrogel

https://dx.doi.org/10.1021/jacs.0c10065
J. Am. Chem. Soc. XXXX, XXX, XXX−XXX

formation within the crystals. These experiments were carried out in the presence of 4 M NaCl to prevent crystal expansion during polymerization. As previously shown,[30] the inclusion of chemical cross-linkers like *N,N′*-methylenebis(acrylamide) was unnecessary for the formation of a stable hydrogel owing to the extensive interactions between the ferritin surface and the carboxylate functional groups of pA, which yield a tightly interwoven physical network.

In a typical expansion experiment, the rhombohedral ^{RAFT}ferritin PIX were transferred into deionized water and monitored by light microscopy for 1−20 min (Figure 3a). The expansion proceeded rapidly upon transfer and followed biphasic kinetics ($\tau_{fast} \leq 10$ s; $\tau_{slow} > 50$ s), with the PIX growing to nearly 200% of their original dimensions within 1 min (Figure 3b). When the same experiments were repeated with propionate, a nonpolymerizable acrylate analog, no expansion was observed, confirming that the pA polymer matrix was responsible for the reversible expansion of PIX (Figure S7). Although microcracks were sometimes visible during pA-induced expansion/contraction, the faceted crystal morphology was preserved throughout the process. Upon addition of NaCl and/or $CaCl_2$, the rhombohedral PIX contracted and regained their original dimensions within 5 s (Figure 3a,b). The expansion/contraction process was fully reversible over at least eight cycles as long as the expansion was stopped before 2 min (Figure S8).

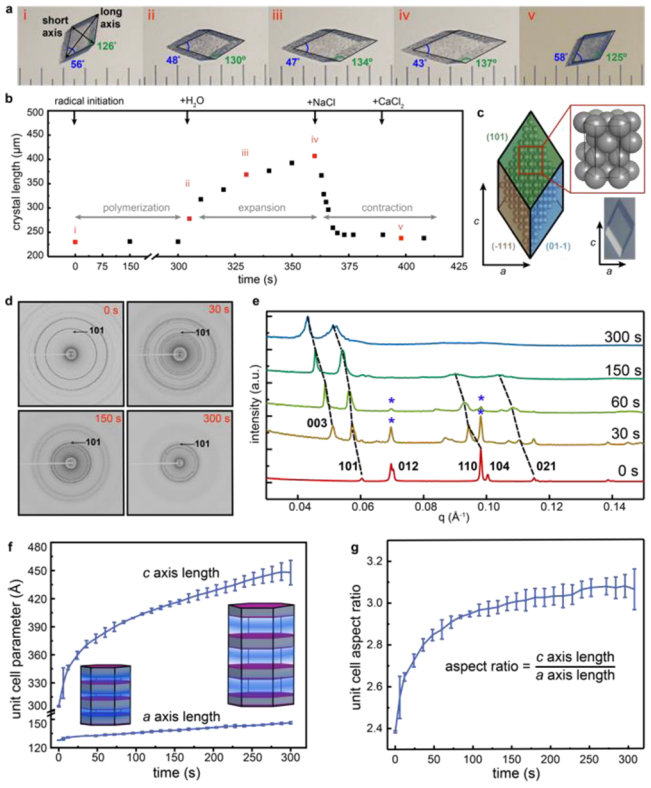

Figure 3. Anisotropic expansion and contraction behavior of rhombohedral ^{RAFT}ferritin PIX. (a) Monitoring of the anisotropic expansion and contraction of a single rhombohedral ^{RAFT}ferritin PIX by light microscopy. The separation between the major ticks of the ruler is 100 μm. (b) The corresponding changes in long-axis length of the same ^{RAFT}ferritin PIX during polymerization, expansion, and contraction. (c) Facet indices and lattice orientation in rhombohedral ^{RAFT}ferritin PIX. (d) SAXS images collected at different time points during the expansion of rhombohedral ^{RAFT}ferritin PIX and (e) the corresponding 1D SAXS profiles. The progression of peaks to lower angles (due to expansion of the unit cell) is indicated with black dashed lines. Peaks corresponding to the original lattice (due to unexpanded crystals) are visible throughout the process and designated with blue asterisks. (f) Changes in the unit cell dimensions of rhombohedral PIX during expansion, calculated from the SAXS profiles shown in part e. (g) Changes in the aspect ratio (i.e., the anisotropy) of the unit cell of rhombohedral PIX during expansion. Error bars: standard deviation of triplicate measurements.

Importantly, the structural dynamics of rhombohedral ^{RAFT}ferritin PIX were highly anisotropic, as evidenced by (a) the increase in the macroscopic aspect ratio of the crystals (defined as $\frac{long\ axis\ length}{short\ axis\ length}$) by over 50% after 1 min of expansion and (b) concomitant changes in the facet angles from ∼56° and ∼126° to ∼43° and ∼137°, respectively (Figure 3a and Video S2). In contrast to rhombohedral PIX, the expansion and contraction of cubic ^{RAFT}ferritin PIX were isotropic at all times (Figure S9), suggesting that directional dynamics do not stem simply from RAFT-polymerization *per se* but likely from the higher density of the pA network in the interlayer interfaces containing the RAFT agents within the rhombohedral ferritin crystals. Indeed, upon assignment of crystal facet indices, we found that the long crystal axis, which showed disproportionate elongation compared to the short axis, aligned with the *c*-axis of the lattice along which the interlayer interfaces were oriented (Figure 3c).

To elucidate lattice dynamics in molecular detail, we carried out time-dependent, small-angle X-ray scattering (SAXS) measurements on ^{RAFT}ferritin PIX. In these experiments, *in-crystallo* polymerization was initiated by X-ray irradiation, and the diffraction patterns of >100 PIX suspended in sample capillaries were collected. The SAXS symmetry was retained (Figure 3d,e). As in the case of light microscopy measurements, the continuous increase in anisotropy during crystal expansion was clearly evident in symmetry was retained (Figure 3d,e). As in the case of light microscopy measurements, the continuous increase in anisotropy during crystal expansion was clearly evident in the diffraction patterns. The unit cell became $a = b = 134.5$ Å, $c = 383.5$ Å after 1 min of expansion, corresponding to an increase in the microscopic aspect ratio (defined as $\frac{c\ axis\ length}{a\ axis\ length}$) by 25% and the cell volume by 43% (Figure 3e,f). After 5 min expansion, the long-range ferritin periodicity was still apparent from the presence of strong (003) and (101) peaks, which yield a unit cell of $a = b = 147.4$ Å, $c = 436.9$ Å (Figure 3d,e). These values correspond to increases in the cell aspect ratio and volume by 31% and 96%, respectively, compared to unexpanded crystals (Figure 3f,g). Consistent with light microscopy measurements, the kinetics for the growth of unit cell dimensions and the increase in longitudinal anisotropy was also nonmonotonic (Figure 3e,f). We attribute this behavior to a fast initial expansion of the dense pA network throughout the PIX, which attenuates as the overall polymer density decreases and polymer chain mobility increases. Time-dependent SAXS measurements were repeated for cubic ^{RAFT}ferritin PIX, which confirmed that the cubic symmetry—thus the 3D isotropy—was retained throughout expansion (Figure S10).

Taken together, our observations are consistent with an anisotropic distribution of the pA polymer matrix within rhombohedral ^{RAFT}ferritin crystals, which we (originally) attributed to a combination of two factors: (1) the specific

https://dx.doi.org/10.1021/jacs.0c10065
J. Am. Chem. Soc. XXXX, XXX, XXX−XXX

interlayer positions of the RAFT agents which promote localized polymer growth and (2) the wide, weakly bound interlayer interfaces, which are further enlarged upon soaking with acrylate monomers. Both factors would lead to the interlayer zones developing a denser matrix of pA polymer compared to the tighter interfaces along the *ab*-planes, thus generating a lamellar pattern (Figure 4a). Consequently, the hydration of the PIX produces a larger extent of lattice expansion parallel to the *c*-axis compared to that in the *ab*-plane (Figure 4a). Although the pA network displays varying densities, it is continuous throughout the mesoporous lattice and forms extensive interactions with the ferritin molecules. The resulting dense mold thus allows the expanded ferritin lattice to fully revert to its original dimensions upon NaCl/$CaCl_2$-induced dehydration. In fact, the sc-XRD measurements show that ^{RAFT}ferritin PIX fully regains near-atomic-level crystallinity upon contraction after 5 min of expansion (Figure 4b), meaning that ferritin molecules can return to their original lattice positions and orientations after having separated from one another by >20 Å in the *ab*-plane and >40 Å along the *c*-axis.

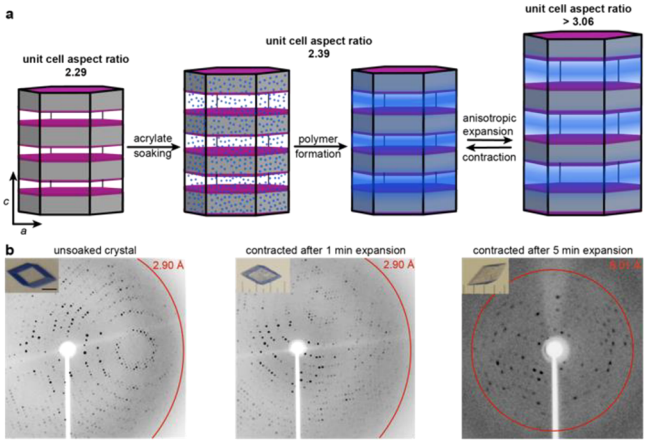

Figure 4. Anisotropic expansion/contraction of rhombohedral ^{RAFT}-ferritin PIX is enabled by the anisotropic polymer matrix and is fully reversible. (a) Schematic summary for the generation of the anisotropic/layered pA network within rhombohedral ^{RAFT}ferritin crystals, which dictates the anisotropic structural dynamics. (b) sc-XRD image (at T = 298 K) of native rhombohedral ^{RAFT}ferritin crystal (left), compared to those of a PIX contracted after 1 min of expansion (middle), and after 5 min of expansion (right). The diffraction limits are indicated with red circles. Light micrographs of the crystals are shown in the insets; the scale bar and separation between the major ticks of the ruler are 100 μm.

Structural Basis of Anisotropic Polymer Distribution in Ferritin PIX. We next examined if the anisotropic pA distribution in ^{RAFT}ferritin PIX indeed could be ascribed to localized polymer growth originating from the RAFT agents on ferritin surfaces. To this end, the ^{RAFT}ferritin PIX were dissolved by treatment with ethylenediaminetetraacetic acid (EDTA) and analyzed by SDS-PAGE and GPC. Interestingly, these ^{RAFT}ferritin PIX samples showed no evidence of covalent attachment between pA chains and ferritin molecules when *in-crystallo* polymerization was induced with APS/TEMED and only minimal yields of graft-from polymerization when VA-044 was used as a radical initiator (Figure S11). The drastically diminished graft-from polymerization efficiencies are likely due to the steric occlusion of the RAFT agents within the interlayer interfaces and slower molecular diffusion within the crystals. These observations implied that the inherent anisotropy of the rhombohedral crystals was alone responsible for templating an anisotropic hydrogel network in ferritin PIX.

An appropriate control system to test this possibility would be ferritin crystals that are also rhombohedral but lack

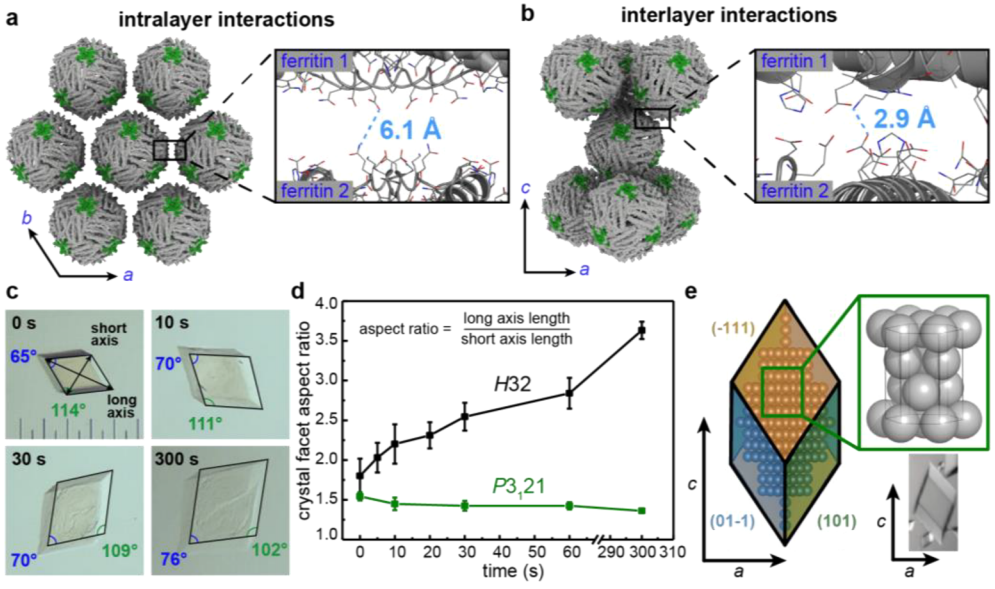

Figure 5. Structural properties and anisotropy of $^{\Delta C}$ferritin crystals/PIX with $P3_121$ symmetry. (a) $^{\Delta C}$ Ferritin molecules along the *ab*-plane are devoid of any intralayer interactions. The closest side chains, Q86 and D84, are 6.1 Å apart which precludes any salt-bridge interactions. (b) Interlayer interactions, oriented along the *c* axis, are mediated by surfaces that include hydrophobic patches. The closest noncovalent interaction is within 3.0 Å and formed by side chains K119 and E116. Where the *H*32 lattice hydrophobic patches would be are highlighted in green. (c) Light micrographs of $P3_121$ symmetric PIX during expansion in water. The separation between the major ticks of the ruler is 100 μm. (d) Changes in the crystal facet aspect ratios of $P3_121$ and *H*32 symmetric PIX during expansion display their respective anisotropic behavior. Error bars: standard deviation of triplicate measurements. (e) Facet indices and lattice orientation in trigonal $^{\Delta C}$ferritin PIX.

https://dx.doi.org/10.1021/jacs.0c10065
J. Am. Chem. Soc. XXXX, XXX, XXX−XXX

covalently attached RAFT agents. Since the RAFT agents are directly involved in lattice packing interactions, we were not able to obtain isomorphous rhombohedral crystals using unmodified ^{C157}ferritin. Yet, in the course of exhaustive screening, we found that a ferritin variant lacking Cys157 (termed ΔC) formed lattices with trigonal symmetry ($P3_121$; $a = b = 131.8$ Å, $c = 301.8$ Å, PDB ID: 7K26) and a rhombohedron-shaped crystal habit that is nearly identical to that of rhombohedral (i.e., $H32$-symmetric) ^{RAFT}ferritin crystals. The 2.7-Å resolution structure of the trigonal crystals indeed revealed a similar hexagonal-layered packing arrangement with an interstitial solvent content of 44.5% but also indicated that the protein interfaces in these lattices substantially differ from those in their rhombohedral counterpart. Notably, the lattice packing interactions between ferritin molecules are mediated entirely by the interlayer interfaces directed along the *c* axis, whereas the intralayer interfaces in the *ab*-plane are *ca.* 6 Å wide at their narrowest point and devoid of direct ferritin-ferritin contacts (Figure 5a,b). Thus, in terms of the orientation of interstitial voids that can be filled with the pA matrix, the trigonal and rhombohedral lattices are orthogonal to one another.

Despite the relative mechanical fragility of the trigonal crystals, we were able to find conditions to form pA matrices within them (Supporting Information). The expansion/contraction properties of the resulting PIX were examined by light microscopy, which revealed that they also displayed anisotropic dynamics, but the direction of crystal expansion was orthogonal to that observed with rhombohedral ^{RAFT}ferritin PIX (Figure 5c–e and Video S3). Whereas the rhombohedral PIX elongated to assume a lozenge shape (with the acute facet angles decreasing from ∼60° to ∼45°, Figure 3a) upon expansion, the trigonal PIX expanded toward a more square-like shape (with the acute facet angles increasing from ∼60° to 76°, Figure 5c), with the overall aspect ratios of the two systems moving in opposite directions (Figure 5d). These findings establish that 1) the anisotropy of the crystal lattices and the underlying orientation/structure of the protein–protein interfaces alone are sufficient for the formation of anisotropic hydrogel networks within PIX, and 2) they can be used to control the directionality of PIX dynamics.

Anisotropic Mechanical and Self-Healing Properties of Rhombohedral ^{RAFT}Ferritin PIX. Analogous to the mechanical anisotropy of muscles enabled by their underlying anisotropic architecture, the directional alignment of polymer chains or embedded particles within hydrogels have been shown to yield anisotropic mechanical properties with respect to the direction of applied force and generate bending motions.[34,35] This behavior was also borne out in expanded rhombohedral ^{RAFT}ferritin PIX, which possess an alternating pattern of high- and low-molecular density regions aligned along the *c*-axis (Figure 6). When the expanded PIX were exposed to Ca^{2+} ions to induce contraction, they underwent a drastic bending motion toward the direction of Ca^{2+} influx, with flexion angles of up ∼25° in the absence of any apparent cracking. The PIX reverted to the original shape as the Ca^{2+} flux dissipated (Figure 6a and Video S4). The bending of the PIX arises from the compression of the hydrogel matrix perpendicular to the hexagonal ferritin *ab*-layers at the Ca^{2+} diffusion front and provides, in essence, a chemosensory/chemotactic motion (Figure 6b). The actuation is remarkably rapid with a bending rate of >10° s^{-1}, which is one-to-several

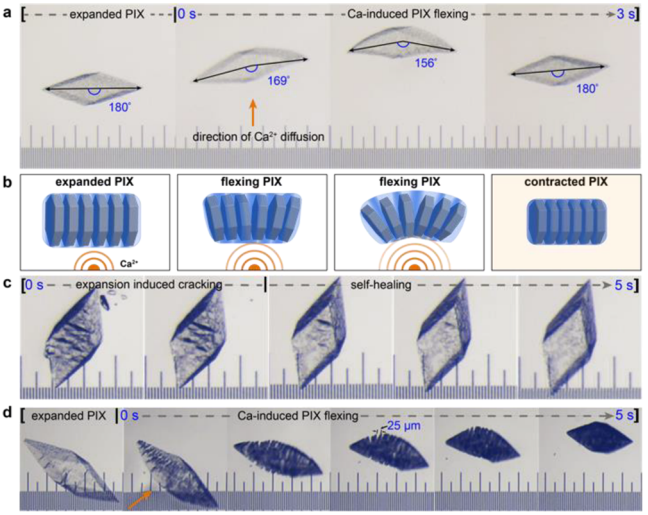

Figure 6. Anisotropic mechanical and self-healing behavior of rhombohedral ^{RAFT}ferritin PIX. (a) Light micrographs showing the bending motion of an expanded ^{RAFT}ferritin PIX flexing in response to Ca^{2+} flux (oriented along the orange arrow). The separation between the major ticks of the ruler in all images is 100 μm. (b) Schematic description for the cation-induced bending motion of the rhombohedral ^{RAFT}ferritin PIX due to the underlying hexagonal-layered lattice arrangement and the anisotropic distribution of the polymer network. (c) Defects in rhombohedral ^{RAFT}ferritin PIX are overwhelmingly oriented in the direction of the *ab*-planes (orthogonal to the long crystal axis) and often spontaneously healed. (d) ^{RAFT}ferritin PIX can undergo susbtantial lamellar fracturing and accordion-like flexing motions in response to Ca^{2+} flux.

orders of magnitude higher than those of recently reported supramolecular and hydrogel systems with some of the fastest reported actuation rates (1.5° s^{-1} and 0.14° min^{-1}, respectively).[49,50] The rapid actuation by the PIX can be ascribed to the high packing density and the structural cooperativity of the integrated crystal-pA matrix.

Under certain circumstances like excessive bending or fast expansion/contraction, the rhombohedral ^{RAFT}ferritin PIX were observed to develop large fractures, sometimes >75 μm in length and >10 μm in width (Figure 6c and Video S5). Consistent with the mechanical anisotropy of these materials, the defects were overwhelmingly oriented along the short crystal axis (i.e., parallel to the hexagonal ferritin layers in the *ab*-planes) (Figure 6c). Owing to the mobility of the hydrogel matrix and its reversible interactions with the ferritin molecules, these large defects were often scarlessly and autonomously healed. In extreme cases, such as that shown in Figure 6d and Video S4, the rhombohedral PIX could even undergo near-complete lamellar fracturing and accordion-like motions to adapt to Ca^{2+} fluxes in solution, followed by full recovery of their original polyhedral morphology within seconds. Such rapid, adaptive motions with attendant self-healing are more typical of soft biological devices like muscles rather than stiff molecular crystals.

CONCLUSIONS

Ranging from abalone nacre and mussel byssus to spider silk and skeletal muscles, nature uses the hierarchical assembly of multicomponent materials to simultaneously achieve a combination of vital properties (e.g., strength, toughness, flexibility, damage tolerance) that would be impossible to obtain through the self-assembly of single components

https://dx.doi.org/10.1021/jacs.0c10065
J. Am. Chem. Soc. XXXX, XXX, XXX–XXX

alone.[51,52] Accordingly, we have shown here that through the physical integration of two disparate classes of materials, i.e., molecular crystals and hydrogel polymers, we can obtain an unprecedented combination of material attributes and mechanical behaviors: atomic-level order/coherence, directional motion, flexibility, rapid anisotropic actuation, chemical responsiveness, self-healing.

Key to the attainment of anisotropic properties in PIX was the ability of ferritin molecules to form lattices with distinct symmetries and protein−protein interfaces. These differences allowed the templation of alternatively patterned hydrogel networks *in situ*, which ultimately enabled ferritin crystals that essentially possess the same macroscopic morphologies to display orthogonally directed motions. The original intent of this study was to achieve control over the spatial distribution of polymer networks within protein crystals using site-directed RAFT-polymerization strategies. Although our findings revealed that such strategies were not necessary to create patterned hydrogels *in crystallo*, we posit they would still offer important advantages if their efficiencies can be improved, such as the incorporation of polymers with a diverse range of functional groups into protein lattices (regardless of their chemical compatibility with the protein components), construction of multipolymer networks, and spatiotemporal control over polymer growth within lattices. Combined with the inherent chemical versatility and functions of proteins, such covalently hybridized PIX could offer a unique platform for the study of protein−polymer interactions and the development of biocatalytic and molecular encapsulation/delivery systems with tunable and responsive mechanical properties.

■ ASSOCIATED CONTENT

Supporting Information

The Supporting Information is available free of charge at https://pubs.acs.org/doi/10.1021/jacs.0c10065.

(PDF)

In-crystallo formation of the hydrogel network monitored by pyranine quenching (MOV)

Structural dynamics of a rhombohedral ^{RAFT}ferritin PIX during polymerization, expansion, and contraction (MOV)

Structural dynamics of a trigonal $^{\Delta C}$ferritin PIX during polymerization, expansion, and contraction (MOV)

Examples of flexing motions in rhombohedral ^{RAFT}ferritin PIX (MOV)

Examples of self-healing behavior in rhombohedral ^{RAFT}ferritin PIX (MOV)

■ AUTHOR INFORMATION

Corresponding Author

F. Akif Tezcan − *Department of Chemistry and Biochemistry and Materials Science and Engineering, University of California, San Diego, La Jolla, California 92093, United States;* orcid.org/0000-0002-4733-6500; Email: tezcan@ucsd.edu

Authors

Kenneth Han − *Department of Chemistry and Biochemistry, University of California, San Diego, La Jolla, California 92093, United States*

Jake B. Bailey − *Department of Chemistry and Biochemistry, University of California, San Diego, La Jolla, California 92093, United States*

Ling Zhang − *Department of Chemistry and Biochemistry, University of California, San Diego, La Jolla, California 92093, United States*

Complete contact information is available at: https://pubs.acs.org/10.1021/jacs.0c10065

Notes

The authors declare no competing financial interest.

Coordinate and structure factor files have been deposited into the RCSB databank under the following PDB IDs: 6WYF, cubic ^{RAFT}ferritin; 6WYG, rhombohedral ^{RAFT}ferritin; 6WYH, Ac-infused rhombohedral ^{RAFT}ferritin; 7K26, Ac-infused trigonal $^{\Delta C}$ferritin.

■ ACKNOWLEDGMENTS

We thank the following colleagues for assistance: R. Alberstein and R. Subramanian for data processing and helpful discussions; A. Rheingold, H. Nguyen, and M. Gembicky for XRD; I. Rajkovic for SAXS; W.J. Rappel for confocal microscopy. This work was funded by the US Army Research Office (W911NF-19-1-0228) for materials design and structural/mechanical characterization. Additional funding was provided by US Department of Energy (BES, Division of Materials Sciences, Biomolecular Materials Program, DE-SC0003844) for SAXS studies and the initial development of the PIX concept. Crystallographic data were collected at Stanford Synchrotron Radiation Lightsource (SSRL), Advanced Light Source (ALS) and the Crystallography Facility of the University of California, San Diego. SAXS data were collected at SSRL. SSRL and ALS are supported by the DOE Office of Science, Office of Basic Energy Sciences under contracts DE-AC02-76SF00515 and DE-AC02-05CH11231, respectively.

■ REFERENCES

(1) Seeman, N. C.; Belcher, A. M. Emulating biology: Building nanostructures from the bottom up. *Proc. Natl. Acad. Sci. U. S. A.* **2002**, *99*, 6451−6455.

(2) Kushner, A. M.; Guan, Z. Modular Design in Natural and Biomimetic Soft Materials. *Angew. Chem., Int. Ed.* **2011**, *50* (39), 9026−9057.

(3) Barthelat, F.; Yin, Z.; Buehler, M. J. Structure and mechanics of interfaces in biological materials. *Nat. Rev. Mater.* **2016**, *1* (4), 16007.

(4) Buehler, M. J.; Yung, Y. C. Deformation and failure of protein materials in physiologically extreme conditions and disease. *Nat. Mater.* **2009**, *8* (3), 175−188.

(5) Naumov, P.; Chizhik, S.; Panda, M. K.; Nath, N. K.; Boldyreva, E. Mechanically Responsive Molecular Crystals. *Chem. Rev.* **2015**, *115* (22), 12440−12490.

(6) Sato, O. Dynamic molecular crystals with switchable physical properties. *Nat. Chem.* **2016**, *8* (7), 644−656.

(7) Suzuki, Y.; Cardone, G.; Restrepo, D.; Zavattieri, P. D.; Baker, T. S.; Tezcan, F. A. Self-assembly of coherently dynamic, auxetic, two-dimensional protein crystals. *Nature* **2016**, *533* (7603), 369−373.

(8) Alberstein, R.; Suzuki, Y.; Paesani, F.; Tezcan, F. A. Engineering the entropy-driven free-energy landscape of a dynamic nanoporous protein assembly. *Nat. Chem.* **2018**, *10* (7), 732−739.

(9) Horike, S.; Shimomura, S.; Kitagawa, S. Soft porous crystals. *Nat. Chem.* **2009**, *1* (9), 695−704.

(10) Schneemann, A.; Bon, V.; Schwedler, I.; Senkovska, I.; Kaskel, S.; Fischer, R. A. Flexible metal-organic frameworks. *Chem. Soc. Rev.* **2014**, *43* (16), 6062−6096.

(11) Ghosh, S.; Reddy, C. M. Elastic and Bendable Caffeine Cocrystals: Implications for the Design of Flexible Organic Materials. *Angew. Chem., Int. Ed.* **2012**, *51* (41), 10319−10323.
(12) Karothu, D. P.; Mahmoud Halabi, J.; Li, L.; Colin-Molina, A.; Rodríguez-Molina, B.; Naumov, P., Global Performance Indices for Dynamic Crystals as Organic Thermal Actuators. *Adv. Mater.*, 1906216.
(13) Kobatake, S.; Takami, S.; Muto, H.; Ishikawa, T.; Irie, M. Rapid and reversible shape changes of molecular crystals on photo-irradiation. *Nature* **2007**, *446* (7137), 778−781.
(14) Mason, J. A.; Oktawiec, J.; Taylor, M. K.; Hudson, M. R.; Rodriguez, J.; Bachman, J. E.; Gonzalez, M. I.; Cervellino, A.; Guagliardi, A.; Brown, C. M. Methane storage in flexible metal-organic frameworks with intrinsic thermal management. *Nature* **2015**, *527* (7578), 357−361.
(15) Sato, H.; Kosaka, W.; Matsuda, R.; Hori, A.; Hijikata, Y.; Belosludov, R. V.; Sakaki, S.; Takata, M.; Kitagawa, S. Self-Accelerating CO Sorption in a Soft Nanoporous Crystal. *Science* **2014**, *343* (6167), 167−170.
(16) Couck, S.; Denayer, J. F. M.; Baron, G. V.; Rémy, T.; Gascon, J.; Kapteijn, F. An Amine-Functionalized MIL-53 Metal-Organic Framework with Large Separation Power for CO_2 and CH_4. *J. Am. Chem. Soc.* **2009**, *131* (18), 6326−6327.
(17) Chen, Q.; Chang, Z.; Song, W. C.; Song, H.; Song, H. B.; Hu, T. L.; Bu, X. H. A controllable gate effect in cobalt (II) organic frameworks by reversible structure transformations. *Angew. Chem., Int. Ed.* **2013**, *52* (44), 11550−11553.
(18) Takashima, Y.; Martínez, V. M.; Furukawa, S.; Kondo, M.; Shimomura, S.; Uehara, H.; Nakahama, M.; Sugimoto, K.; Kitagawa, S. Molecular decoding using luminescence from an entangled porous framework. *Nat. Commun.* **2011**, *2* (1), 168.
(19) McKinlay, A. C.; Eubank, J. F.; Wuttke, S.; Xiao, B.; Wheatley, P. S.; Bazin, P.; Lavalley, J. C.; Daturi, M.; Vimont, A.; De Weireld, G.; Horcajada, P.; Serre, C.; Morris, R. E. Nitric Oxide Adsorption and Delivery in Flexible MIL-88(Fe) Metal-Organic Frameworks. *Chem. Mater.* **2013**, *25* (9), 1592−1599.
(20) Chen, Q.; Chang, Z.; Song, W.-C.; Song, H.; Song, H.-B.; Hu, T.-L.; Bu, X.-H. A Controllable Gate Effect in Cobalt(II) Organic Frameworks by Reversible Structure Transformations. *Angew. Chem., Int. Ed.* **2013**, *52* (44), 11550−11553.
(21) Panda, M. K.; Ghosh, S.; Yasuda, N.; Moriwaki, T.; Mukherjee, G. D.; Reddy, C. M.; Naumov, P. Spatially resolved analysis of short-range structure perturbations in a plastically bent molecular crystal. *Nat. Chem.* **2015**, *7* (1), 65−72.
(22) Serre, C.; Mellot-Draznieks, C.; Surblé, S.; Audebrand, N.; Filinchuk, Y.; Férey, G. Role of Solvent-Host Interactions That Lead to Very Large Swelling of Hybrid Frameworks. *Science* **2007**, *315* (5820), 1828−1831.
(23) Worthy, A.; Grosjean, A.; Pfrunder, M. C.; Xu, Y.; Yan, C.; Edwards, G.; Clegg, J. K.; McMurtrie, J. C. Atomic resolution of structural changes in elastic crystals of copper(II) acetylacetonate. *Nat. Chem.* **2018**, *10*, 65−69.
(24) Commins, P.; Al-Handawi, M. B.; Karothu, D. P.; Raj, G.; Naumov, P. Efficiently self-healing boronic ester crystals. *Chem. Sci.* **2020**, *11* (10), 2606−2613.
(25) Commins, P.; Hara, H.; Naumov, P. Self-Healing Molecular Crystals. *Angew. Chem., Int. Ed.* **2016**, *55* (42), 13028−13032.
(26) Wei, Y.-S.; Chen, K.-J.; Liao, P.-Q.; Zhu, B.-Y.; Lin, R.-B.; Zhou, H.-L.; Wang, B.-Y.; Xue, W.; Zhang, J.-P.; Chen, X.-M. Turning on the flexibility of isoreticular porous coordination frameworks for drastically tunable framework breathing and thermal expansion. *Chem. Sci.* **2013**, *4* (4), 1539−1546.
(27) Pang, J.; Wu, M.; Qin, J.-S.; Liu, C.; Lollar, C. T.; Yuan, D.; Hong, M.; Zhou, H.-C. Solvent-Assisted, Thermally Triggered Structural Transformation in Flexible Mesoporous Metal-Organic Frameworks. *Chem. Mater.* **2019**, *31* (21), 8787−8793.
(28) Zhang, Y. S.; Khademhosseini, A. Advances in engineering hydrogels. *Science* **2017**, *356* (6337), No. eaaf3627.
(29) Jeon, S.-J.; Hauser, A. W.; Hayward, R. C. Shape-Morphing Materials from Stimuli-Responsive Hydrogel Hybrids. *Acc. Chem. Res.* **2017**, *50* (2), 161−169.
(30) Zhang, L.; Bailey, J. B.; Subramanian, R. H.; Groisman, A.; Tezcan, F. A. Hyperexpandable, self-healing macromolecular crystals with integrated polymer networks. *Nature* **2018**, *557* (7703), 86−91.
(31) Theil, E. C. Ferritin: structure, gene regulation, and cellular function in animals, plants, and microorganisms. *Annu. Rev. Biochem.* **1987**, *56* (1), 289−315.
(32) Huard, D. J.; Kane, K. M.; Tezcan, F. A. Re-engineering protein interfaces yields copper-inducible ferritin cage assembly. *Nat. Chem. Biol.* **2013**, *9* (3), 169−76.
(33) Lawson, D. M.; Artymiuk, P. J.; Yewdall, S. J.; Smith, J. M.; Livingstone, J. C.; Treffry, A.; Luzzago, A.; Levi, S.; Arosio, P.; Cesareni, G.; Thomas, C. D.; Shaw, W. V.; Harrison, P. M. Solving the structure of human H ferritin by genetically engineering intermolecular crystal contacts. *Nature* **1991**, *349* (6309), 541−4.
(34) Sano, K.; Ishida, Y.; Aida, T. Synthesis of Anisotropic Hydrogels and Their Applications. *Angew. Chem., Int. Ed.* **2018**, *57* (10), 2532−2543.
(35) Park, N.; Kim, J. Hydrogel-Based Artificial Muscles: Overview and Recent Progress. *Adv. Intell. Sys.* **2020**, *2* (4), 1900135.
(36) Chiefari, J.; Chong, Y. K.; Ercole, F.; Krstina, J.; Jeffery, J.; Le, T. P. T.; Mayadunne, R. T. A.; Meijs, G. F.; Moad, C. L.; Moad, G.; Rizzardo, E.; Thang, S. H. Living Free-Radical Polymerization by Reversible Addition-Fragmentation Chain Transfer: The RAFT Process. *Macromolecules* **1998**, *31* (16), 5559−5562.
(37) Boyer, C.; Bulmus, V.; Davis, T. P.; Ladmiral, V.; Liu, J.; Perrier, S. Bioapplications of RAFT Polymerization. *Chem. Rev.* **2009**, *109* (11), 5402−5436.
(38) De, P.; Li, M.; Gondi, S. R.; Sumerlin, B. S. Temperature-Regulated Activity of Responsive Polymer-Protein Conjugates Prepared by Grafting-from via RAFT Polymerization. *J. Am. Chem. Soc.* **2008**, *130* (34), 11288−11289.
(39) Cobo, I.; Li, M.; Sumerlin, B. S.; Perrier, S. Smart hybrid materials by conjugation of responsive polymers to biomacromolecules. *Nat. Mater.* **2015**, *14* (2), 143−159.
(40) Akcora, P.; Liu, H.; Kumar, S. K.; Moll, J.; Li, Y.; Benicewicz, B. C.; Schadler, L. S.; Acehan, D.; Panagiotopoulos, A. Z.; Pryamitsyn, V.; Ganesan, V.; Ilavsky, J.; Thiyagarajan, P.; Colby, R. H.; Douglas, J. F. Anisotropic self-assembly of spherical polymer-grafted nanoparticles. *Nat. Mater.* **2009**, *8* (4), 354−359.
(41) Lu, C.; Urban, M. W. Stimuli-responsive polymer nano-science: Shape anisotropy, responsiveness, applications. *Prog. Polym. Sci.* **2018**, *78*, 24−46.
(42) Yu, Y.; Nakano, M.; Ikeda, T. Directed bending of a polymer film by light. *Nature* **2003**, *425* (6954), 145−145.
(43) Jiang, S.; Liu, F.; Lerch, A.; Ionov, L.; Agarwal, S. Unusual and Superfast Temperature-Triggered Actuators. *Adv. Mater.* **2015**, *27* (33), 4865−4870.
(44) Erb, R. M.; Sander, J. S.; Grisch, R.; Studart, A. R. Self-shaping composites with programmable bioinspired microstructures. *Nat. Commun.* **2013**, *4* (1), 1712.
(45) Liu, M.; Ishida, Y.; Ebina, Y.; Sasaki, T.; Hikima, T.; Takata, M.; Aida, T. An anisotropic hydrogel with electrostatic repulsion between cofacially aligned nanosheets. *Nature* **2015**, *517* (7532), 68−72.
(46) Chin, S. M.; Synatschke, C. V.; Liu, S.; Nap, R. J.; Sather, N. A.; Wang, Q.; Álvarez, Z.; Edelbrock, A. N.; Fyrner, T.; Palmer, L. C.; Szleifer, I.; Olvera de la Cruz, M.; Stupp, S. I. Covalent-supramolecular hybrid polymers as muscle-inspired anisotropic actuators. *Nat. Commun.* **2018**, *9* (1), 2395.
(47) Qin, H.; Zhang, T.; Li, N.; Cong, H.-P.; Yu, S.-H. Anisotropic and self-healing hydrogels with multi-responsive actuating capability. *Nat. Commun.* **2019**, *10* (1), 2202.
(48) Yu, J.; Wang, Q.; O'Hare, D.; Sun, L. Preparation of two dimensional layered double hydroxide nanosheets and their applications. *Chem. Soc. Rev.* **2017**, *46* (19), 5950−5974.

https://dx.doi.org/10.1021/jacs.0c10065
J. Am. Chem. Soc. XXXX, XXX, XXX−XXX

(49) Chen, J.; Leung, F. K.-C.; Stuart, M. C. A.; Kajitani, T.; Fukushima, T.; van der Giessen, E.; Feringa, B. L. Artificial muscle-like function from hierarchical supramolecular assembly of photo-responsive molecular motors. *Nat. Chem.* **2018**, *10* (2), 132−138.
(50) Iwaso, K.; Takashima, Y.; Harada, A. Fast response dry-type artificial molecular muscles with [c2]daisy chains. *Nat. Chem.* **2016**, *8* (6), 625−632.
(51) Fratzl, P.; Weinkamer, R. Nature's hierarchical materials. *Prog. Mater. Sci.* **2007**, *52* (8), 1263−1334.
(52) Espinosa, H. D.; Rim, J. E.; Barthelat, F.; Buehler, M. J. Merger of structure and material in nacre and bone - Perspectives on de novo biomimetic materials. *Prog. Mater. Sci.* **2009**, *54* (8), 1059−1100.

https://dx.doi.org/10.1021/jacs.0c10065
J. Am. Chem. Soc. XXXX, XXX, XXX−XXX